한 국 방 재 학 회 논 문 집
제8권 6호 2008년 12월
pp. 1 ~ 5

건축방재

Temperature Compensation Technique for Steel Sleeve Packaged FBG Strain Sensor and Its Application in Structural Monitoring

Yun, Ying-wei* · Jang, Il-Young**

Abstract

As bare Fiber Bragg Grating (FBG) sensors are very fragile, bare FBG without encapsulation is not properly applied in practical infrastructures directly due to the harsh environment in practical engineering. Steel sleeve packaged FBG strain sensor is widely used in civil engineering. Since FBG senses both strain and temperature simultaneously, for accurate measurement of strain, temperature compensation for FBG strain sensors is indispensable. In this paper, based on the FBG's strain and temperature sensing principles, the temperature compensation techniques for steel sleeve packaged FBG sensors are brought forward. And the experiment of concrete early-age shrinkage monitoring by dual FBG sensors is carried out to test the feasibility of the temperature compensation technique.

***Key words* : Steel sleeve packaged FBG strain sensor, sensing mechanism, temperature compensation, structural monitoring**

요 지

피복이 없는 FBG센서는 내구성이 매우 약하기 때문에 FBG센서 주위의 피복이 없이는, 많은 변수가 존재하는 실제 자연환경에서의 정확한 데이터수집이 어렵다. Steel sleeve packaged FBG 변형률 센서는 토목공학에서 널리 사용되고 있는 센서 중 하나이다. 변형률과 온도가 동시에 측정되는 FBG센서의 도입 이후로, 변형률과 온도의 정확한 보정은 필수적인 과정이 되었다. 이 논문에서는 FBG의 변형률과 온도의 측정 원리에 기초하여 steel sleeve packaged FBG센서의 온도보정 기술을 도출하였다. 그리고 두개의 FBG센서를 이용한 콘크리트 초기재령의 건조수축 실험을 통해 온도보정의 실행 가능성을 확인하였다.

핵심용어 : Steel sleeve packaged FBG 변형률 센서, 감응원리, 온도보정, 구조물 모니터링

1. Introduction

Structural Health Monitoring (SHM) has currently become the highlight of researches and applications in civil engineering. And its challenge is damage detection and identification. Local damage monitoring seems paramount. Generally speaking, local damage behaves as crack, fatigue, slip, debonding, stiffness loss, effective force-resistance area loss, and so on. Strain is an alternative parameter which can be used to describe deformation, study the crack opening and even detect the slip and bonding, so high-quality strain sensor, which shows advantages of stability and durability, has always been desirable. The fiber Bragg grating (FBG) sensor, one of the optical fiber sensors has more and more been the focus for strain sensor in structural health monitoring due to its distinguished merits such as good resistance to electromagnetic interference, small size, good corrosion resistance and multiplexing technique. FBG strain sensor has now been widely studied and applied in infrastructures, since Hill et.al. (1978) and Meltz et al. (1989) developed the FBG fabrication techniques. However, due to the fact that bare FBG sensors are very fragile, bare FBG without encapsulation is not properly applied in practical infrastructures directly because it can not adapt to the rudeness of construction. Therefore packaged FBG sensors are developed for construction application. Steel sleeve packaged FBG strain sensor is one of the widely used sensors in civil engineering. Since FBG senses both strain and temperature simultaneously, for accurate measurement of strain, temperature compensation for FBG strain sensor is indispensable. Many researches have been done on temperature compensation methods for FBG strain sensor, which include two main methods: compensation method based on measurement process and compensation according to measurement result. Compensation method based on measurement process is that temperature effect is eliminated by special arrangement and design of sensing units, which include dual-parameter measurement (Xu, M. G. et al., 1994), using opposite temperature expansion materials(Iwashima, T. et al., 1997), Chirped Bragg grating (Xu, M. G, et al.,1995), etc. Considering the complex fabrication technique of this method, it is not proper for practical applications. However, compensation method according to measurement result has just been done based on bare FBG sensor, and its application

*Lecturer in Luoyang Institute of Science and Technology (China) & PhD candidate in Kumoh National Institute of Technology (Korea), (E-mail: zhongguoren@kumoh.ac.kr)
**Member · Professor in Civil and Environmental Engineering Dept. · Kumoh National Institute of Technology

is only limited in laboratory use due to fragility. Even applied in construction site, the installing method is pretty complicated due to the harsh environment which may damage the bare FBG sensors (Zhou, Zhi. et al, 2004).

In this paper, based on the FBG's strain and temperature sensing principles, the temperature compensation technique for steel sleeve packaged FBG strain sensor are brought forward. And the experiment of concrete early-age shrinkage monitoring by dual FBG sensors'is carried out to test the feasibility of the temperature compensation technique.

2. Sensing mechanism of FBG on strain and temperature

When broadband light passes through the FBG, the narrow-band spectral component at the Bragg wavelength is reflected by the FBG as shown Fig. 1. The basic principle of FBG's is to measure the shift of reflected Bragg wavelength (λ_B), which is related to the effective refraction index (n_{eff}) and the period (Λ) of the index variation of the grating area in fiber core. The Bragg wavelength is given by:

$$\lambda_B = 2n_{eff}\Lambda \tag{1}$$

The shift of Bragg grating wavelength can be expressed as Eq.(2) by differentiating Eq.(1):

$$d\lambda_B = 2n_{eff}d\Lambda + 2\Lambda dn_{eff} \tag{2}$$

Any perturbation that can change effective index (n_{eff}) and period (Λ) will result in a shift of Bragg wavelength. Strain and temperature are such perturbations, on which structural health monitoring has focused.

2.1 FBG strain sensing property

Here only the wavelength shift of Bragg grating due to strain perturbation is considered. Combination of Eq.(1) and Eq.(2) yields:

$$\frac{d\lambda_B}{\lambda_B} = \frac{d\Lambda}{\Lambda} + \frac{dn_{eff}}{n_{eff}} \tag{3}$$

where $\frac{d\Lambda}{\Lambda}$ is strain (ε). $\frac{dn_{eff}}{n_{eff}}$ induced by strain (ε) can be expressed as

$$\frac{dn_{eff}}{n_{eff}} = -\frac{n_{eff}^2}{2}[p_{12} - v(p_{11} + p_{12})]\varepsilon \tag{4}$$

where p_{11} and p_{12} are Pockel's coefficients of strain-optical tensor, and v is Poisson's ratio.

Given, $P = [p_{12} - v(p_{11} + p_{12})]n_{eff}^2/2$, then Eq.(5) is obtained:

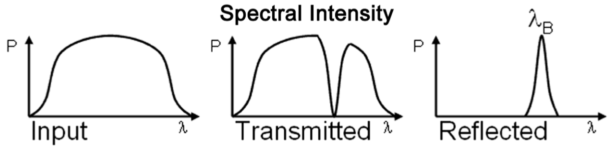

Fig 1. Schemes of sensing mechanism for fiber Bragg gratings

$$d\lambda_B = \lambda_B(1-P)\varepsilon = \alpha_\varepsilon\varepsilon \tag{5}$$

where α_ε is strain sensitivity of fiber Bragg gratings. Eq.(5) is the relationship between FBG wavelength shift and strain without considering temperature change.

2.2 FBG temperature sensing property

When FBG is affected by temperature, the changes of period and effective refraction index induced by temperature will result in wavelength shift of Bragg grating. By introducing temperature change (dT) in Eq.(2), Eq.(6) can be derived as:

$$d\lambda_B = 2\left(n_{eff}\frac{d\Lambda}{dT} + \Lambda\frac{dn_{eff}}{dT}\right)dT \tag{6}$$

From Eq.(6) and Eq.(1), we have

$$\frac{d\lambda_B}{\lambda_B} = \left(\frac{1}{\Lambda}\frac{d\Lambda}{dT} + \frac{1}{n_{eff}}\frac{dn_{eff}}{dT}\right)dT \tag{7}$$

where $\frac{1}{\Lambda}\frac{d\Lambda}{dT} = \alpha$ is thermal expansion coefficient of FBG sensor, and $\zeta = \frac{dn_{eff}}{dT}$ is the thermal optical constant, Eq.(7) can be rewritten as:

$$d\lambda_B = \lambda_B\left(\alpha + \frac{\zeta}{n_{eff}}\right)dT \tag{8}$$

Let $\alpha_T = \lambda_B\left(\alpha + \frac{\zeta}{n_{eff}}\right)$ be temperature sensitivity coefficient of fiber Bragg gratings, and then Eq.(8) can be simplified as follows:

$$d\lambda_B = \alpha_T dT \tag{9}$$

If fiber Bragg grating is subjected to strain and temperature simultaneously, the wavelength shift can be express as Eq.(10) without considering the coupling effect between temperature and strain:

$$d\lambda_B = \alpha_\varepsilon\varepsilon + \alpha_T dT \tag{10}$$

3. Temperature compensation for steel sleeve packaged FBG strain sensors

In the practical application of FBG sensor in civil engineering, protection measures ought to be done due to the fragility of bare FBG sensor. Generally, bare FBG is encapsulated in steel sleeve as shown in Fig. 2. Once bare FBG sensor is encapsulated by steel sleeve, its thermal performance will change when subject to stress together with the structures that it measures. Next, the Bragg wavelength shift of embedded-steel sleeve packaged FBG strain

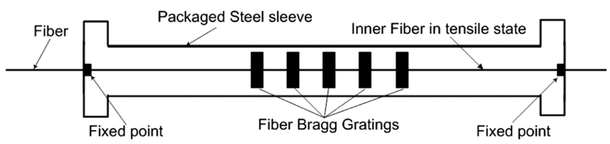

Fig 2. The scheme of embedded steel-sleeve packaged FBG strain sensor

sensor under co-action of stain and temperature is derived.

Fig. 2 is the scheme of embedded-steel packaged FBG strain sensor. The inner FBG fiber is tensioned tightly between the two ends of the steel sleeve, which ensures that the deformations of fiber and steel sleeve are compatible. As temperature difference dT occurs, the interactive force F will happen between fiber and steel sleeve due to their different thermal expansion coefficients. The strain of steel sleeve ε_s can be expressed as:

$$\varepsilon_s = -\frac{F}{A_s E_s} + \alpha_s dT \tag{11}$$

where A_s is the cross-section area of steel sleeve, E_s is its elastic modulus, and α_s is its thermal expansion coefficient. Correspondingly, the strain of fiber ε_f is:

$$\varepsilon_f = \frac{F}{A_f E_f} + \alpha_f dT \tag{12}$$

where A_f is the cross-section area of fiber, E_f is its elastic modulus, and α_f is its thermal expansion coefficient. As the deformations of steel sleeve and fiber are compatible, then

$$\varepsilon_s = \varepsilon_f \tag{13}$$

By combining Eqs.(11),(12) with (13), F can be solved:

$$F = (\alpha_s - \alpha_f)dT \frac{A_s E_s A_f E_f}{A_s E_s + A_f E_f} \tag{14}$$

Substitute Eq.(14) into Eq.(12), then ε_f can be obtained as Eq.(15):

$$\varepsilon_f = (\alpha_s - \alpha_f)dT \frac{A_s E_s}{A_s E_s + A_f E_f} + \alpha_f dT \tag{15}$$

As $A_s E_s \gg A_f E_f$, Eq.(15) can be rewritten:

$$\varepsilon_f = \alpha_s dT \tag{16}$$

According to Eq.(16), fiber strain due to temperature change is determined by the thermal performance of the packaging steel sleeve. When steel sleeve packaged FBG sensor is embedded in concrete structure for measurements, thermal deformation of fiber itself due to temperature can be neglected as thermal expansion coefficient of packaged sensor is similar with that of concrete. Therefore, fiber strain of embedded sensor due to temperature is thought as the concrete thermal strain.

The wavelength shift of FBG embedded in the concrete structures is composed of two parts: (1) wavelength shift due to structural strain ε, which includes structural strain ε_0 subject to loading and the structural strain $\alpha_c dT$ due to temperature change dT, where α_c is the thermal expansion coefficient of concrete. (2) wavelength shift resulting from temperature varying, as the thermal deformation of fiber itself can be neglected, here only the effective refractive index varying due to thermal effect is considered (thermal sensitive effect). Then according to Eq.(10), the wavelength shift of embedded strain sensor can be expressed as:

$$d\lambda_B = \alpha_\varepsilon(\varepsilon_0 + \alpha_c dT) + \alpha_T dT \tag{17}$$

For temperature compensation for FBG strain senor, a FBG temperature sensor is placed in the vicinity of it, which only responds to the temperature change while no response for deformation due to its special structure. The scheme of FBG temperature sensor is shown in Fig. 3. For FBG temperature sensor, the inner FBG fiber is in relaxed state which ensures that it is only sensitive to temperature change.

Under the co-action of structural strain and temperature varying, wavelength shift of FBG strain sensor and that of FBG temperature sensor are expressed as below:

$$\begin{cases} d\lambda_{B1} = \alpha_{\varepsilon 1}\varepsilon + \alpha_{T1} dT \\ d\lambda_{B2} = \alpha_{T2} dT \end{cases} \tag{18}$$

where subscript 1 and 2 denote FBG strain sensor and temperature sensor, respectively. By solving Eq.(18), we can get

$$\varepsilon = \frac{d\lambda_{B1} - \frac{\alpha_{T1}}{\alpha_{T2}} d\lambda_{B2}}{\alpha_{\varepsilon 1}} \tag{19}$$

Introducing $\varepsilon = \varepsilon_0 + \alpha_c\, dT$ into Eq.(19), then ε_0 can be obtained as:

$$\varepsilon_0 = \frac{d\lambda_{B1} - \frac{\alpha_{T1}}{\alpha_{T2}} d\lambda_{B2}}{\alpha_{\varepsilon 1}} - \frac{\alpha_c}{\alpha_{T2}} d\lambda_{B2} \tag{20}$$

Eq.(20) can be rewritten as:

$$\varepsilon_0 = \frac{d\lambda_{B1}}{\alpha_{\varepsilon 1}} - \left(\frac{\alpha_{T1}}{\alpha_{\varepsilon 1}} + \alpha_c\right)\frac{d\lambda_{B2}}{\alpha_{T2}} \tag{21}$$

Based on above Eqs. (19) and (21), we can get the accurate strain from the measured FBG wavelength easily.

4. Application in monitoring the early age shrinkage of concrete beam and discussions

High-rise apartment construction works are built in Yongin City as shown in Fig. 4(a). And the measured beam is cast by ready mixed HPC. Steel-sleeve packaged Embedded FBG strain sensor and FBG temperature sensor from Micro Optics Co. (USA) are used in this research. Fig. 4(b) shows the detailed position of embedded FBG sensors which are installed in the middle span of concrete beam due to the possible micro-cracking during loading period in future test. And the FBG temperature sensor should be installed closely to FBG strain sensor inside the beam so that they are located in the same temperature field for temperature compensation. Sensitivity coefficients of FBG sensors used in

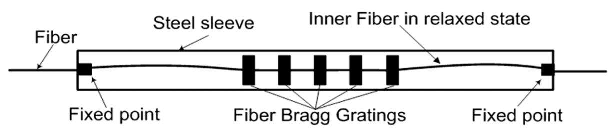

Fig 3. Scheme of Steel packaged FBG temperature sensor

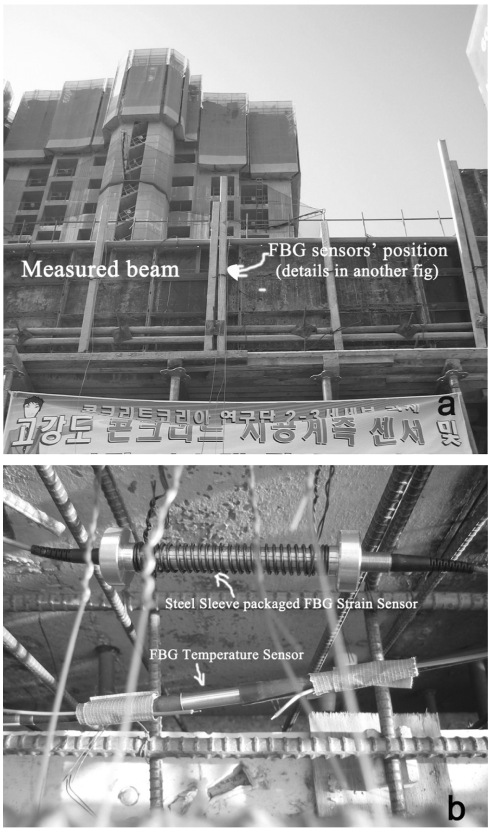

Fig 4. (a) the measured beam in construction site (b) the installed FBG sensors inside the concrete beam

this research are shown in Table. 1. To acquire and process the measurand-induced signal from each sensor, an optical sensing interrogator- sm130-500 made by Micron Optics, Inc is used (included in Fig. 5) based on wavelength division multiplexing (WDM) technique. Fig. 5 shows the monitoring system used in this in-situ application.

In the early age of concrete pouring, rapid variation of concrete temperature is observed from FBG temperature sensor in Fig. 6 due to the large amount of hydration heat released by cement hydrating. Fig. 7 presents the concrete strain varying curves before and after temperature compensation, which shows that temperature compensation for FBG strain sensor is imperative to get accurate strain data especially when temperature changes rapidly.

Table 1. Sensitivity coefficient of FBG sensors

Type of sensor	λ (nm)	Strain Co. $\alpha_\varepsilon(pm/\mu\varepsilon)$	Temp Co. $\alpha_t(pm/{}^{o}C)$
Temp sensor	1528.9	/	8.8
Strain sensor	1539.4	1.5	25.0

Fig 5. FBG monitoring system used in this application

Before initial setting of concrete, the elastic modulus of concrete paste tends to zero. During this liquid concrete phase there is no structure to hold the body firmly in place. Any movement due to applied stresses will be immediately corrected by a shift in the position of the body. Therefore, during this stage, the deformation of concrete (also called chemical shrinkage) can be neglected for long term durability of structures. After initial setting, Young's modulus of concrete will rapidly increase, and skeleton to resist stress will form, which implies that concrete deformation is restricted. Aïctin, P.C pointed out that the start of autogenous shrinkage is from initial setting time (Aïctin, P.C., 1999), which is used as a reference value. Hence, monitoring concrete deformation from initial setting time is important for control possible micro cracks in concrete structures. In this research, needle penetration tests were applied to predict the initial setting time of premixed HPC-- initial setting is about 8 hrs after concrete pouring.

As there is no loading on the concrete beam at its early age, the total strain of concrete beam ε includes:

$$\varepsilon = \varepsilon_{thermal} + \varepsilon_{drying} + \varepsilon_{carbonation} + \varepsilon_{autogenous} \tag{22}$$

where $\varepsilon_{thermal}$ is thermal strain of concrete. The thermal expansion coefficient of concrete after initial setting is adopted as $1.2 \times 10^{-5}/{}^{o}C$, and concrete thermal strain equals $\alpha_c dT$.

ε_{drying} is the drying shrinkage of concrete beam, which is con-

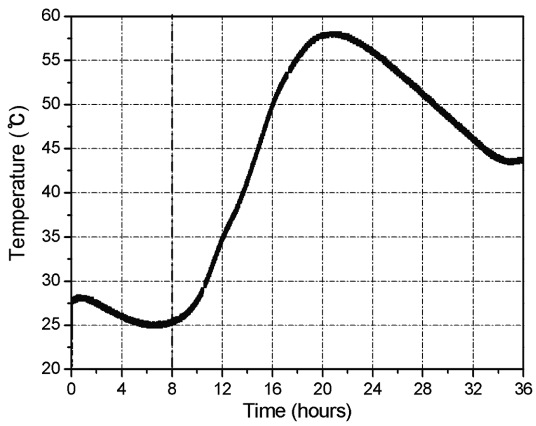

Fig 6. Concrete hydration temperature varying within the first 36 hours after concrete pouring

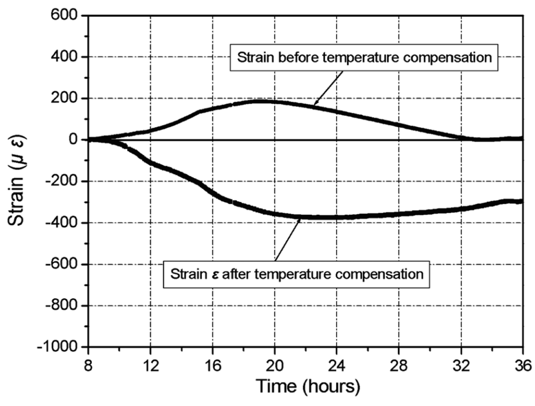

Fig 7. Concrete strain within the first 36 hours from initial setting with & without temperature compensation

sidered negligible here due to the fact that evaporation was prevented by the covered plastic sheet during curing period.

$\varepsilon_{carbonation}$ is carbonation shrinkage which is caused by the reaction of the hydrated cement paste with the carbon dioxide in the air when humidity is present. In the early age time and within the short period this deformation is also neglected.

$\varepsilon_{autogenous}$ is autogenous shrinkage which refers to the reduction of available water for hydration caused as the consequence of the hydration process itself. Therefore, Eq.(22) can be rewritten as:

$$\varepsilon = \varepsilon_0 \,(= \varepsilon_{autogenous}) + \alpha_c dT \tag{23}$$

According to Eqs.(17) and (19), total strain of concrete beam before and after temperature compensation are shown in Fig. 7. By comparing the specimens strain before temperature compensation with that after temperature compensation, it can be found that the inner strain of HPC beam obtained from FBG strain sensor directly is obviously wrong due to the fact that the micro strain should not reach such high degree and always be tension strain in early age. Whereas, after temperature compensation, the results show very reasonable, which proves that it is necessary to make temperature compensation when FBG strain sensors serve in structural monitoring system. According to Eq.(23), concrete autogenous shrinkage and thermal strain can be obtained as shown in Fig. 8, which shows that high autogenous shrinkage in the early age of HPC agrees with the results of Tazawa E. and Miyazawa S(1993). The maximal autogenous shrinkage is up to 800 $\mu\varepsilon$, which is much larger than that of ordinary concrete in the literature of Davis H.E. (1940). Therefore, autogenous shrinkage of high performance concrete should be emphasized in practical constructions.

5. Conclusions

Based on the FBG's strain and temperature sensing principles, the temperature compensation techniques for steel sleeve packaged FBG sensors are put forward. For steel sleeve packaged FBG sensor embedded in concrete structure, thermal deformation of fiber itself due to temperature change can be neglected as thermal expansion coefficient of packaged sensor is similar to that of concrete. Therefore, fiber strain of embedded sensor due to temperature is thought as the concrete thermal strain. And the developed compensation technique is used to monitor early age deformation and temperature of HPC beam member in construction site, which nicely verifies the feasibility and practicability of the temperature compensation technique. Meanwhile, the results show that in the early age of concrete pouring, temperature compensation for FBG strain sensor is urgently imperative to get accurate concrete strain measure as the violent cement hydration leads to great temperature change. Also, the conclusion that autogenous shrinkage of HPC at early age is much larger than that of ordinary concrete is demonstrated.

The temperature compensation technique for steel sleeve packaged FBG strain sensor put forward in this paper is feasible to be extended to structure health monitoring in civil engineering, such as concrete dams, large span bridges, high-rise buildings or large infrastructures etc.

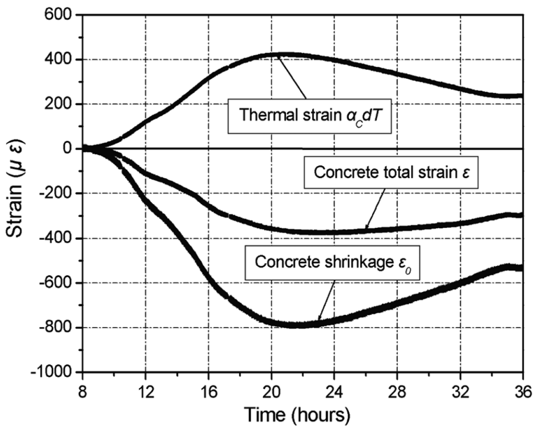

Fig 8. Concrete thermal strain, total strain and autogenous shrinkage within the first 36 hours from initial setting

6. Acknowledgements

This research was funded by Center for Concrete Corea (05-CCT-D11), supported by KMOCT (Korea Ministry of Construction & Transportation). The financial support is gratefully acknowledged.

References

Aïctin, P.C. (1999) *Autogenous Shrinkage of Concrete.* edited by Tazawa, E., E & FN Spon, pp. 257-268.

Davis H.E. (1940) Autogenous volume change of concrete. *Proceeding of the 43rd Annual American Society for Testing Materials*, Atlantic City, ASTM, pp. 1103-1113.

Hill, K. O., Fujii, Y., Johnson D.C. et al. (1978) Photosensitivity in optical fiber waveguides: application to reflection fiber fabrication. *Appl. Phys. Lett.* Vol. 32, No. 10, pp. 647-649.

Iwashima, T., Inoue, A., Shigematsu, M. *et al*. (1997) Temperature compensation technique for fiber Bragg grating using liquid crystalline polymer tubes. *Electronics letters*, Vol. 33, No. 5, pp. 417-419.

Meltz, G., Morey, W. W and Glenn, W. H. (1989) Formation of Bragg gratings in optical fibers by a transverse holographic method. *Opt. Lett.* Vol. 14, No. 15, pp.823-825.

Tazawa E. and Miyazawa S.(1993) Autogenous shrinkage of concrete and its importance in concrete technology, in: Z.P. Bazant, L. Carol (Eds.), *Creep and Shrinkage of Concrete, Proceedings of the 5th International RILEM Symposium*, E & FN Spon, London, pp. 159-168.

Xu, M.G., Archambault J.L., Reekei L. ,et al.(1994) Discrimination between strain and temperature effects using dual-wave length fiber grating sensors. *Electronics letters*, Vol. 30, No.13, pp.1085-1087.

Xu, M. G., Dong, L. and Reekie, L. et al. (1995) Temperate-independent strain sensor using a chirped Bragg grating in a tapered optical fiber. *Electronics Letters*, Vol.31, pp.823-825.

Zhou Zhi and OU Jinping. (2004) Techniques of temperature compensation for FBG strain sensors. *Proceeding of Asian Pascifc Fundamental Problems of Opto- and Microelectronics (APCOM 2004)*, Khabarovsk, Russia, pp.465-471

◎ 논문접수일 : 08년 08월 28일
◎ 심사의뢰일 : 08년 09월 02일
◎ 심사완료일 : 08년 11월 28일